Local Strength of Single-Coped Beams

BO DOWSWELL

ABSTRACT

In beam-to-beam connections, the top flange of the supported beam is usually coped to clear the supporting beam flange. Due to flexural and shear stresses in the coped portion of the web, the local strength can be limited by buckling. Design recommendations in previous editions of the AISC *Manual* imposed limits on the cope geometry and were based on an allowable stress philosophy, limiting the flexural strength to the first-yield moment. To eliminate the limits of applicability and provide equations that take advantage of any available post-yield strength, the design guidance in the 15th Edition AISC *Steel Construction Manual* has been revised from previous editions of the AISC *Manual*. This paper discusses the development of the revised design procedure and validates the equations with the results of 25 experimental tests from five independent research projects.

Keywords: single-coped beams, AISC *Steel Construction Manual*, steel connections, post-yield strength.

INTRODUCTION

In beam-to-beam connections, the top flange of the supported beam is usually coped to clear the supporting beam flange as shown in Figure 1. The cope length can be large at skewed beam connections, connections to wide flange truss chords, and other framing conditions. Due to flexural and shear stresses in the coped portion of the web, the local strength can be limited by buckling.

Design recommendations in previous editions of the AISC *Steel Construction Manual* (AISC, 2011) were developed by Cheng and Yura (1986) based on a local buckling model with an adjustment factor determined by curve fitting data from finite element models. Because the adjustment factor was derived empirically, limits of applicability, based on the maximum cope size modeled, were placed on the design equations. The design procedure is not valid if the cope length exceeds twice the beam depth or the cope depth exceeds 50% of the beam depth. In some practical cases, the cope geometry falls outside these limits of applicability.

Stress concentrations at the reentrant corner, shown in Figure 2, were considered by Cheng and Yura (1986) in the formulation of their equations for web buckling. For flexural yielding calculations, Cheng and Yura recommended that localized yielding due to stress concentrations be neglected. The flexural strength is the minimum of the web buckling moment and the first yield moment. This methodology was common for stress-based design; however, a strength-based design philosophy is now preferred.

To eliminate the limits of applicability and provide equations that take advantage of any available inelastic strength, the design guidance in the 15th Edition *Steel Construction Manual* (AISC, 2017) has been revised from previous editions of the *Manual*. This paper discusses the development of the revised design procedure and validates the equations with the results of 25 experimental tests from five independent research projects.

Bo Dowswell, Ph.D., P.E., Principal, ARC International, Birmingham, AL. Email: bo@arcstructural.com

Paper No. 2017-19

REVISED DESIGN PROCEDURE

The revised design procedure for the local flexural strength of single-coped beams is on page 9-6 of the 15th Edition *Manual*. The available flexural strength, $\phi_b M_n$ or M_n/Ω_b, of a beam coped at the top flange must equal or exceed the required strength. For beams with compression-flange lateral bracing at the face of the cope, the required flexural strength is:

LRFD	ASD
$M_u = R_u e$ (AISC *Manual* Eq. 9-5a)	$M_a = R_a e$ (AISC *Manual* Eq. 9-5b)

For beams coped at the top flange, the connection element should be located near the coped edge. The minimum length of the connection element is one-half of the coped section depth, h_o. The nominal flexural strength of the coped section is:

When $\lambda \le \lambda_p$

$$M_n = M_p \qquad \text{(AISC } \textit{Manual} \text{ Eq. 9-6)}$$

When $\lambda_p < \lambda \le 2\lambda_p$

$$M_n = M_p - (M_p - M_y)\left(\frac{\lambda}{\lambda_p} - 1\right) \qquad \text{(AISC } \textit{Manual} \text{ Eq. 9-7)}$$

When $\lambda_p > 2\lambda_p$

$$M_n = F_{cr} S_{net}$$

(AISC *Manual* Eq. 9-8)

where

$$F_{cr} = \frac{0.903 E k_1}{\lambda^2}$$ (AISC *Manual* Eq. 9-9)

$$k_1 = fk \geq 1.61$$ (AISC *Manual* Eq. 9-10)

$$\lambda = \frac{h_0}{t_w}$$ (AISC *Manual* Eq. 9-11)

$$\lambda_p = 0.475\sqrt{\frac{k_1 E}{F_y}}$$ (AISC *Manual* Eq. 9-12)

The plate buckling coefficient, k, is determined as follows:

When $\frac{c}{h_0} \leq 1.0$

$$k = 2.2\left(\frac{h_0}{c}\right)^{1.65}$$

(AISC *Manual* Eq. 9-13a)

When $\frac{c}{h_0} > 1.0$

$$k = 2.2\frac{h_0}{c}$$

(AISC *Manual* Eq. 9-13b)

The buckling adjustment factor, f, is determined as follows:

When $\frac{c}{d} \leq 1.0$

$$f = 2\left(\frac{c}{d}\right)$$

(AISC *Manual* Eq. 9-14a)

When $\frac{c}{d} > 1.0$

$$f = 1 + \frac{c}{d} \leq 3$$

(AISC *Manual* Eq. 9-14b)

where

E = modulus of elasticity, ksi
F_{cr} = critical stress, ksi
F_y = specified minimum yield stress, ksi
M_p = plastic bending moment, kip-in.
$= F_y Z_{net}$
M_y = flexural yield moment, kip-in.
$= F_y S_{net}$
R_a = required end reaction for ASD, kips
R_u = required end reaction for LRFD, kips
S_{net} = elastic section modulus at the cope, in.^{3}
Z_{net} = plastic section modulus at the cope, in.^{3}
c = cope length, in.
d = beam depth, in.
e = distance from the face of the supporting member to the face of the cope, unless a lower value can be justified, in.
f = buckling adjustment factor
h_0 = depth of the coped section, in.
k = plate buckling coefficient
k_1 = modified plate buckling coefficient
t_w = web thickness, in.
λ = web slenderness
λ_p = limiting slenderness for a compact web
Ω_b = 1.67
ϕ_b = 0.90

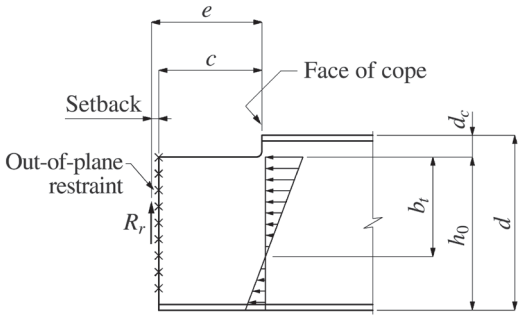

Fig. 1. Single-coped beam.

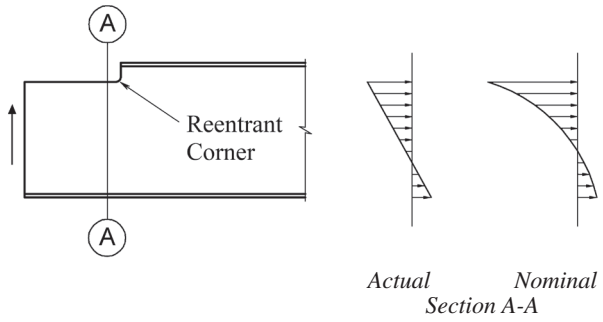

Fig. 2. Local flexural stress at the cope face.

EXISTING RESEARCH

A review of the available research on single-coped beams revealed 25 experimental tests from five previously published research projects. The details of all test specimens are listed in Table A1 of Appendix A, and the experimental results are listed in Tables A2 and A3.

Birkemoe and Gilmor

As part of a larger project, Birkemoe and Gilmor (1978) tested one beam coped at the top flange with bolted clip angles. At the maximum test load, the holes were highly deformed and the tension plane between the bottom bolt and the end of the beam ruptured. Some localized buckling was observed at the top edge of the cope, but it is unclear if the buckling occurred before, or after, the tension-plane rupture.

Ricles and Yura

The results of unpublished experiments by Ricles and Yura are documented in Appendix B of Cheng et al. (1984). The failure mode of all four tests was inelastic web local buckling.

Cheng and Yura

Cheng and Yura (1986) developed the design procedure recommended in previous editions of the AISC *Manual*. The equations were based on the plate buckling model shown in Figure 3, with the flexural stresses idealized using a triangular normal stress distribution along both loaded edges. The top edge was restraint free, and the remaining three edges were fixed against translation but rotationally free. A buckling adjustment factor was developed using a finite element based parametric study that included the effects of stress concentration, shear stress, out-of-plane translation of the reentrant corner, moment gradient over the length of the cope, and rotational restraint of the web at the face of the cope.

Ten experiments were used to verify the design model. Four of the specimens failed by inelastic buckling and six failed by elastic buckling. Compared to these 10 tests along with the four unpublished tests by Ricles and Yura, the equations were shown to be conservative but adequate for design purposes.

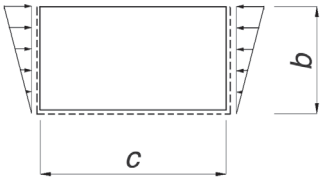

Fig. 3. Plate buckling model.

Yam et al.

Based on a shear buckling model, Yam et al. (2003) developed a set of design equations that accurately predicted the failure loads of four experimental specimens. The critical end reaction is:

$$R_{cr} = \tau_{cr} t_w h_0 \tag{1}$$

The critical shear stress is:

$$\tau_{cr} = \frac{\pi^2 E k_s}{12(1-\nu^2)}\left(\frac{t_w}{h_0}\right)^2 \tag{2}$$

The plate buckling coefficient in shear is:

$$k_s = a\left(\frac{h_0}{c}\right)^b \tag{3}$$

where

$$a = 1.38 - 1.79\left(\frac{d_c}{d}\right) \tag{4}$$

$$b = 1.55 - 3.66\left(\frac{d_c}{d}\right) + 3.64\left(\frac{d_c}{d}\right)^2 \tag{5}$$

k_s = shear buckling coefficient
τ_{cr} = critical shear stress, ksi
ν = Poisson's ratio

Zhong et al.

Zhong et al. (2004) tested 10 single-coped beam specimens with welded clip angles. Four specimens failed in block shear, and six failed in a combined block shear and cope buckling mode. Only the specimens that buckled are included in Table A1.

Discussion

Three failure modes were identified involving local stability of the web: flexural local buckling, shear buckling, and combined block shear and buckling. Most of the observed failure modes were a combination of shear buckling and flexural local buckling, as indicated by buckled shapes that form a diagonal angle between 0° and 45° from vertical. The buckled shapes reported by Cheng et al. (1984) and Yam et al. (2003) were curved, with the angle from vertical increasing with decreasing cope length.

Flexural local buckling is likely to dominate the buckling mode for beams with long copes. With flexural local buckling, the compression edge of the coped section takes the shape of a half sine wave, which usually extends partially into the uncoped portion of the web due to lateral translation of the web at the reentrant corner.

Shear buckling occurs in beams with short cope lengths. Where shear stresses are predominant, the buckled shape is

similar to that of the well-documented shear buckling waves in non-coped beams. The buckled shape is characterized by a single wave oriented at an angle of approximately 45° from vertical, as shown in Figure 4.

Combined block shear and cope buckling, hereafter referred to as "block shear buckling," occurs at short copes with shallow end connections as shown in Figure 5. The failure is characterized by a combination of extensive yielding along the L-shape block shear failure pattern, with potential rupture at the tension plane and localized buckling at the face of the cope.

DEVELOPMENT OF DESIGN PROCEDURE

The revised design procedure uses a three-part curve, based on the local buckling design model in the AISC *Specification* (2016). Because the buckled shapes most closely resemble flexural local buckling over the critical variable range, the equations developed by Cheng and Yura (1986) were used for elastic portion of the curve. The limits of applicability are eliminated by transitioning to a minimum plate buckling coefficient, which is not affected by the local stress and restraint conditions due to the large cope dimensions.

Analogy to Local Buckling of Tee Stems

For an infinitely long cope, the strength approaches that of a tee stem in flexural compression. However, there are several differences between tee-beams and copes that can significantly affect the behavior:

- For coped beams, the restraint against twisting of the bottom flange provided by the non-coped portion of the beam creates a fixed boundary condition at the web-to-flange interface.
- The moment gradient over the cope length is higher than for a typical beam.
- The shear load is uniform over the cope length; therefore, both the maximum shear and the maximum moment occur at the face of the cope. Typically, the maximum shear and maximum moment in a tee-beam occur at different locations along the beam length. It is generally expected that the shear load carried by a tee-beam will not affect the flexural strength. Conversely, the experimental research shows that very high shear loads can degrade the flexural strength of copes.
- Extensive yielding of copes does not present a serviceability concern. Due to the high shape factor of tee-beams, AISC *Specification* Section F9.1 imposes an upper limit on the flexural yielding strength.
- The residual stress pattern for coped beams can be much different from that of tee-beams. This will be discussed further in the next section.

Due to these factors, AISC *Specification* Section F9.4 for local buckling of tee stems in flexural compression may not be valid for cope buckling calculations.

Residual Stresses

Residual stresses must be considered in the development of the inelastic segment of the strength curve. Most fabrication operations have an effect on the residual stress pattern, but the last operation performed has the greatest influence on the final pattern.

Copes are usually thermally cut, with grinding if required to remove edge imperfections. Thermal cutting causes tensile residual stresses over a small length at the cut edge (Bjorhovde et al., 2001; Harris, 1997). Residual stresses caused by grinding are dependent on several factors, such as wheel speed, abrasive roughness, and use of coolant. In typical structural fabrication shops, handheld angle grinders are used with no coolant, which induces tensile residual stresses upon cooling (Harvey, 1985).

Tension residual stresses at the cut edge can increase the buckling strength of elements subjected to flexural compression stresses. This effect is clearly demonstrated in the research of Bambach and Rasmussen (2002) and Rogers and Dwight (1977). Unlike the local buckling provisions for noncompact elements in AISC *Specification* Chapter F, which were developed for elements with compression residual stresses, residual stresses for coped beams are beneficial. Therefore, they were neglected in the derivation of AISC *Manual* Equation 9-7.

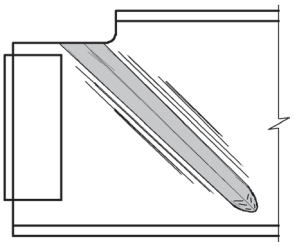

Fig. 4. Shear buckling.

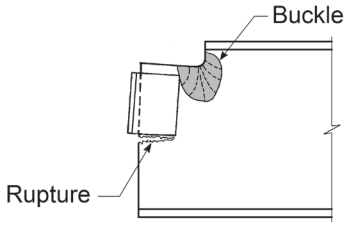

Fig. 5. Block shear buckling.

Buckling Curve

The revised design method uses a three-part curve similar to the local buckling provisions in AISC *Specification* Chapter F. A linear transition between the elastic buckling curve and the plastic strength curve defines the strength when $\lambda_p < \lambda \le \lambda_r$ according to Equation 6:

$$M_n = M_p - (M_p - M_y)\left(\frac{\lambda - \lambda_p}{\lambda_r - \lambda_p}\right) \quad (6)$$

Slenderness Limits

The noncompact slenderness limit, λ_r, can be determined using the critical plate buckling stress according to Equation 7 (Bryan, 1890). For an infinitely long plate with fixed-free boundary conditions at the nonloaded edges and a triangular stress distribution as shown in Figure 3, the plate buckling coefficient, k, is 1.61 (Brockenbrough and Johnston, 1974).

$$\sigma_{cr} = \frac{\pi^2 Ek}{12(1-\nu^2)}\left(\frac{t}{b}\right)^2 \quad (7)$$

where

b = plate width, in.

k = plate buckling coefficient

t = plate thickness, in.

ν = Poisson's ratio

For copes, the width-to-thickness ratio, λ, is defined as h_0/t_w, which is consistent with the AISC *Specification* definition for tee stem buckling. Because only the portion of the web between the neutral axis and the free edge is in compression, this definition is conservative. Based on the current shapes in the AISC *Manual* with the smallest practical cope depth ($d_c = k$), the average value of b_c/h_0 is 0.764, where b_c is the width of the compression region in the web as shown in Figure 1. The standard deviation is 0.0369, and the maximum value of b_c/h_0 for any shape is 0.843.

To estimate the effect of the neutral axis offset, three elastic finite element models of long tee-shaped beams were developed. BASP finite element software was used, as described by Akay et al. (1977), to determine the critical loads. Equal and opposite moments were applied at the ends, and the flange was rotationally fixed against twisting. The cross-sectional dimensions of a W16×26 were used with depths of 8.17 in., 11.17 in. and 14.17 in. The webs buckled in multiple half-wavelengths, indicating that the modeled beam length was appropriate for simulating the behavior of infinitely long copes. Using the current definition for the width-to-thickness ratio ($\lambda = h_0/t_w$), the buckling coefficients calculated with the finite element results are 2.24, 2.34 and 2.42. The average value is 2.33, which is a 45% increase over the theoretical value of 1.61 due to the conservative definition of λ.

Element slenderness values have traditionally been multiplied by a reduction factor, $\alpha = 0.7$, to account for residual stresses and geometric imperfections. Due to the beneficial effect of the residual stress and the conservative definition of λ, $\alpha = 1$ is used in the calculation of the slenderness limit for noncompact webs, λ_r. Using Equation 7, the noncompact limit is

$$\lambda_r = \pi\sqrt{\frac{kE}{12(1-\nu^2)F_y}} = 0.95\sqrt{\frac{kE}{F_y}} \quad (8)$$

To account for the differences between cope buckling and plate buckling, the modified plate buckling coefficient, k_1, developed by Cheng and Yura (1986) was substituted for k, resulting in Equation 9.

$$\lambda_r = 0.95\sqrt{\frac{k_1 E}{F_y}} \quad (9)$$

Because $\lambda_p = \lambda_r/2$ provided the best fit to the experimental data, λ_r was replaced with $2\lambda_p$, which allowed Equation 6 to be simplified, resulting in *Manual* Equation 9-7. Limits on the cope length and depth are eliminated by setting the minimum value of k_1 to 1.61 and limiting f to a maximum value of 3.

Experimental Comparisons

Details of 25 experimental tests from five previously published research projects are listed in Appendix A, Table A1. Three failure modes were identified: localized buckling (LB), shear yielding (VY), and block shear buckling (BB). Most of the specimens failing by localized buckling had characteristics of both shear and flexural buckling. Due to the difficulty distinguishing between shear and flexural local buckling, these failure modes were identified as localized buckling. Where further information was available, either elastic localized buckling (EB) or inelastic localized buckling (IB) was identified.

The experimental results for specimens failing by localized buckling or shear yielding are listed in Table A2. Of these 18 specimens, nine failed by elastic buckling, seven failed by inelastic buckling, and two failed by combined shear yielding and inelastic buckling. Table A2 lists the maximum experimental loads and the experimental failure modes. For each specimen, the calculated load is listed for each of the three design procedures discussed: Cheng and Yura (1986), Yam et al. (2003), and the 15th Edition *Manual* procedure. The calculations utilized the measured material and geometric properties where available. Resistance factors

and safety factors were omitted from the calculations. For each of the three design procedures, the experimental-to-calculated load ratio, R_e/R_c, and predicted failure mode are listed. All three design procedures are reasonably accurate.

In most cases, the revised AISC *Manual* design procedure accurately predicted the experimental failure mode. For the specimens failing in elastic localized buckling, the revised *Manual* procedure and the Cheng and Yura (1986) method produce identical results. The primary difference between the two methods is with the more common case of inelastic localized buckling, where the revised *Manual* equations are more accurate and less conservative. The average experimental-to-calculated load ratio for the revised *Manual* procedure is 1.23 with a standard deviation is 0.267.

The experimental data is plotted in Figure 6 with the three-part curve defined by the revised AISC *Manual* design procedure. Due to the high slenderness of Cheng and Yura's (1986) specimens PB26A and PB26B, the data points fall outside of the range of Figure 6. For the specimens predicted to fail by shear yielding, the vertical-axis values were calculated using an equivalent plastic moment, $M_p = V_y e$, where V_y is the shear yield force calculated with AISC *Specification* Equation J4-3 using the measured material and geometric properties. The experimental data follow the design curve for moderate and high slenderness values; however, three data points fall slightly below the curve in the low-slenderness range. This is caused by the interaction of shear and normal loads, which has the greatest effect on the specimens with short cope lengths, where λ approaches λ_p.

Influence of Inflection Point Location

To reflect the standard practice of neglecting any effect of connection rotational rigidity on the cope strength, e is defined as the "distance from the face of the supporting member to the face of the cope…" However, the second part of the definition, "…unless a lower value can be justified," allows the engineer to determine if a smaller value is appropriate. Because the plate buckling equations developed by Cheng and Yura (1986) include the effects of shear stress and moment gradient over the length of the cope, the validity of calculating the required moment based on an inflection point within the cope (Figure 7) is questionable. Cheng and Yura's (1986) specimens W3 and RB18A illustrate this point.

Specimen W3 had an inflection point 3.9 in. from the beam end (Table A2 in Appendix A), which is 37% of the cope length. With a local slenderness ratio, $\lambda/\lambda_p = 1.51$, as predicted, the specimen failed by inelastic localized buckling. As listed in Table A2, the AISC *Manual* design procedure is 10% conservative when the influence of the inflection point location is neglected. If the required moment is calculated using the actual location of the inflection point, the calculated load is nonconservative, with an experimental-to-calculated load ratio of $R_e/R_c = 0.830$.

For specimen RB18A, the inflection point was 8 in. from the beam end (Table A2 in Appendix A), which is 44% of the cope length. With a local slenderness ratio, $\lambda/\lambda_p = 1.74$, as predicted, the specimen failed by inelastic localized buckling. As listed in Table A2, the AISC *Manual* design

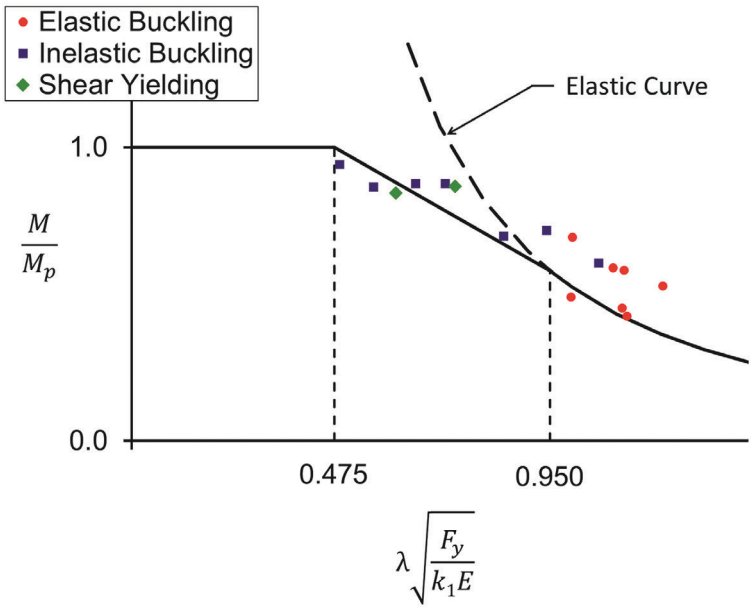

Fig. 6. Normalized moment versus normalized slenderness.

procedure is 27% conservative when the effect of the inflection point is neglected. If the required moment is calculated using the actual location of the inflection point, the calculated load is nonconservative, with an experimental-to-calculated load ratio of $R_e/R_c = 0.600$.

Based on the λ/λ_p ratios, it appears that the inflection point location has a greater effect on less slender copes. Until further research is available, the following design guidance is suggested:

- Generally, e should be defined as the distance from the face of the cope to the end of the beam.
- When $\lambda \le \lambda_p$, the required moment can be calculated using the inflection point location.
- When $\lambda > \lambda_p$, the required moment can be calculated using the inflection point location only if an additional check is made for shear buckling according to Equations 1 through 5.

Block Shear Buckling

The seven specimens that failed by block shear buckling are documented in Table A3. Using the revised AISC *Manual* procedure and *Specification* Sections J4.2 and J4.3, the strength of each specimen was calculated for the limit states of flexure, shear yielding, and block shear. The calculated beam reactions for each of the three limit states are listed in columns 4 through 6, and the minimum of the three calculated values, R_{min}, is listed in column 7. The calculations utilized the measured material and geometric properties where available. Resistance factors and safety factors were omitted from the calculations. For all specimens, the calculated strength was controlled by block shear.

The experimental-to-calculated load ratios, R_e/R_{min}, are listed in column 8 of Table A3. The average experimental-to-calculated load ratio is 1.03 with a standard deviation of 0.126. Although the average value is greater than 1.00, the reliability of this failure mode is lower than for other coped beams failing in a traditional block shear mode with no cope buckling. For coped beams with welded clip angles failing in block shear with no buckling, the average experimental-to-calculated load ratio is 1.24 with a standard deviation of 0.0847. For coped beams with single-row bolted clip angles failing in block shear with no buckling, the average experimental-to-calculated load ratio is 1.37 with a standard deviation of 0.121.

Because all of the specimens failing by block shear buckling had a short connection element depth, L, compared to the depth of the coped section, h_0, it is believed that this failure mode can be eliminated by satisfying $L/h_0 \ge 0.5$. As shown in column 2 of Table A3, the L/h_0 values for all specimens are less than 0.5. For most practical connections this requirement is satisfied by the AISC *Manual* recommendation for erection stability, where the minimum angle length is equal to one-half of the beam T-dimension.

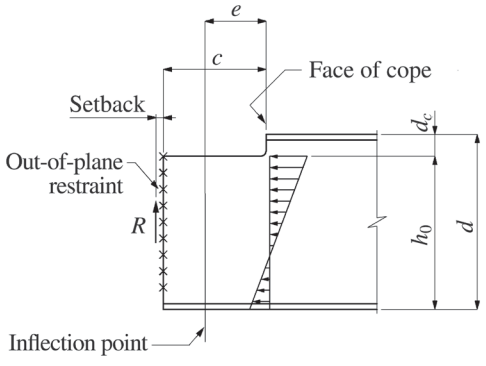

Fig. 7. Eccentricity defined by the inflection point.

CONCLUSIONS

Results from five previously published research projects were used to develop design recommendations for single-coped beams that are consistent with strength design philosophy. The revised design method, which is included in the 15th Edition AISC *Steel Construction Manual* (AISC, 2017), uses a three-part curve similar to the local buckling provisions in AISC *Specification* Chapter F (AISC, 2016). The limitations on cope length and cope depth in the previous *Manual* design procedure are not required with the revised procedure.

For long, slender copes that are controlled by elastic buckling, and for copes that are controlled by shear yielding, the revised design procedure results in the same strength as the previous *Manual* procedure. However, the revised equations utilize the inelastic flexural strength of nonslender copes, which reduces the conservatism and improves the accuracy compared to the previous AISC *Manual* equations.

Of the 25 experiments evaluated, 18 specimens failed by either localized buckling or shear yielding. In most cases, the revised design procedure accurately predicted the experimental failure mode. The average experimental-to-calculated load ratio for the 15th Edition AISC *Manual* procedure is 1.23 with a standard deviation is 0.267.

A new failure mode that combined block shear and cope buckling (block shear buckling) occurred in seven experimental specimens with short copes and shallow end connections. To prevent this limit state, a new geometric limit requires the connection element at the beam end to be at least one-half of the coped section depth.

DESIGN EXAMPLE

Given: Using LRFD design, determine if the cope flexural strength is adequate for a 70-kip factored beam end reaction for the beam shown in Figure 8. The beam material is ASTM A992.

Solution:

From AISC Manual Table 1-1:

W18×35
$t_w = 0.30$ in. $\quad d = 17.7$ in.

From AISC *Manual* Table 9-2: $S_{net} = 18.2$ in.^{3}

From AISC Design Examples V15.0 Table IV-11: $Z_{net} = 32.1$ in.^{3}

$$M_y = F_y S_{net}$$
$$= (50 \text{ ksi})(18.2 \text{ in.}^3)$$
$$= 910 \text{ kip-in.}$$

$$M_p = F_y Z_{net}$$
$$= (50 \text{ ksi})(32.1 \text{ in.}^3)$$
$$= 1{,}610 \text{ kip-in.}$$

$$\frac{c}{d} = \frac{7.5 \text{ in.}}{17.7 \text{ in.}}$$
$$= 0.424$$

Because $\frac{c}{d} < 1.0$, AISC *Manual* Equation 9-14a is applicable:

$$f = 2\left(\frac{c}{d}\right)$$
$$= 2(0.424)$$
$$= 0.847$$

$$\frac{c}{h_0} = \frac{7.5 \text{ in.}}{15.7 \text{ in.}}$$
$$= 0.478$$

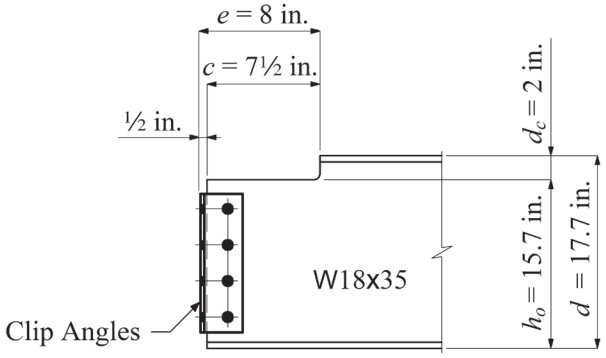

Fig. 8. Design example.

Because $\frac{c}{h_0} < 1.0$, AISC *Manual* Equation 9-13a is applicable:

$$k = 2.2\left(\frac{h_0}{c}\right)^{1.65}$$
$$= 2.2\left(\frac{15.7}{7.5}\right)^{1.65}$$
$$= 7.44$$

$$k_1 = fk \geq 1.61$$
$$= (0.847)(7.44)$$
$$= 6.30$$

$$\lambda = \frac{h_o}{t_w}$$
$$= \frac{15.7\text{ in.}}{0.300\text{ in.}}$$
$$= 52.3$$

$$\lambda_p = 0.475\sqrt{\frac{k_1 E}{F_y}}$$
$$= 0.475\sqrt{\frac{(6.30)(29{,}000\text{ ksi})}{(50\text{ ksi})}}$$
$$= 28.7$$

Because $\lambda_p < \lambda \leq 2\lambda_p$, AISC *Manual* Equation 9-7 is applicable.

$$M_n = M_p - (M_p - M_y)\left(\frac{\lambda}{\lambda_p} - 1\right)$$
$$= 1{,}610\text{ kip-in.} - (1{,}610\text{ kip-in.} - 910\text{ kip-in.})\left(\frac{52.3}{28.7} - 1\right)$$
$$= 1{,}030\text{ kip-in.}$$

$$\phi R_n = \frac{\phi M_n}{e}$$
$$= \frac{(0.90)(1{,}030\text{ kip-in.})}{8\text{ in.}}$$
$$= 116\text{ kips} > 70\text{ kips} \quad \textbf{o.k.}$$

Therefore, the W18×35 coped beam is adequate to resist the 70-kip end reaction.

SYMBOLS

A_{gv} Gross area subjected to shear, in.^{2}
E Modulus of elasticity, ksi
F_{cr} Critical stress, ksi
F_y Specified minimum yield stress, ksi
L Connection element depth, in.
M_a Required flexural strength for ASD, kip-in.
M_p Plastic bending moment, kip-in.
M_u Required flexural strength for LRFD, kip-in.
M_y Flexural yield moment, kip-in.
R_a Required end reaction for ASD, kips
R_r Required end reaction, kips

R_u Required end reaction for LRFD, kips

S_{net} Elastic section modulus at the cope, in.^{3}

V_n Nominal shear yield force, kips

V_r Required shear force, kips

V_y Shear yield force calculated with the measured material and geometric properties, kips

Z_{net} Plastic section modulus at the cope, in.^{3}

b Plate width, in.

b_c Width of the compression region in the web, in.

c Cope length, in.

d Beam depth, in.

d_c Cope depth, in.

e Distance from the face of the supporting member to the face of the cope, unless a lower value can be justified, in.

f Buckling adjustment factor

h_0 Depth of the coped section, in.

k Plate buckling coefficient

k_s Shear buckling coefficient

k_1 Modified plate buckling coefficient

s Web depth dedicated to shear resistance, in.

t Plate thickness, in.

t_f Flange thickness, in.

t_w Web thickness, in.

y_p Distance from the bottom of the beam to the plastic neutral axis, in.

λ Web slenderness

λ_p Limiting slenderness parameter for a compact element

λ_r Limiting slenderness parameter for a noncompact element

Ω_b Safety factor for flexure

Ω_v Safety factor for shear yielding

ϕ_b Resistance factor for flexure

ϕ_v Resistance factor for shear yielding

τ_{cr} Critical shear stress, ksi

ν Poisson's ratio

REFERENCES

AISC (2011), *Steel Construction Manual*, 14th Edition, American Institute of Steel Construction, Chicago, IL.

AISC (2016), *Specification for Structural Steel Buildings*, ANSI/AISC 360-16, American Institute of Steel Construction, Chicago, IL.

AISC (2017), *Steel Construction Manual*, 15th Edition, American Institute of Steel Construction, Chicago, IL.

Akay, H.U., Johnson, C.P. and Will, K.M. (1977), "Lateral and Local Buckling of Beams and Frames," *Journal of the Structural Division,* ASCE, Vol. 103, No. ST9, pp. 1,821–1,832.

Bambach, M.R. and Rasmussen, K.J.R. (2002), "Tests of Unstiffened Elements Under Combined Compression and Bending," Research Report R818, Center for Advanced Structural Engineering, University of Sydney.

Birkemoe, P.C. and Gilmor, M.I. (1978), "Behavior of Bearing Critical Double-Angle Beam Connections," *Engineering Journal*, AISC, Vol. 15 , No. 4, pp. 109–115.

Bjorhovde, R., Engstrom, M.F., Griffis, L.G., Kloiber, L.A. and Malley, J.O. (2001), *Structural Steel Selection Considerations—A Guide for Students, Educators, Designers, and Builders*, American Society of Civil Engineers, Reston, VA.

Brockenbrough, R.L. and Johnston, B.G. (1974), *U.S. Steel Design Manual*, 2nd Edition, U.S. Steel Corporation, Pittsburgh, PA.

Bryan, G.H. (1890), "On the Stability of a Plane Plate under Thrusts in Its Plane, with Applications to the Buckling of the Sides of a Ship," *Proceedings of the London Mathematical Society*, Vol. 22, No. 1, pp. 54–67.

Cheng, J.J. and Yura, J.A. (1986), "Local Web Buckling of Coped Beams," *Journal of Structural Engineering*, ASCE, Vol. 112, No. 10.

Cheng, J.J., Yura, J.A. and Johnson, C.P. (1984), "Design and Behavior of Coped Beam," Ferguson Lab Report, University of Texas at Austin, Austin, TX.

Harris, I.D. (1997), *Plasma Arc Cutting of Bridge Steels*, Report 384, National Cooperative Highway Research Program, National Academy Press, Washington, DC.

Harvey, J.F. (1985), *Theory and Design of Pressure Vessels*, Van Nostrand Reinhold Co., New York, NY.

Rogers, N.A. and Dwight, J.B. (1977), "Outstand Strength," *Steel Plated Structures, An International Symposium*, Granada Publishing LTD.

Yam, M.C.H., Lam, A.C.C., Lu, V.P. and Cheng, J.J.R. (2003), "Local Web Buckling Strength of Coped Steel I Beams," *Journal of Structural Engineering*, ASCE, Vol. 129, No. 1.

Zhong, J.Y.C., Yam, M.C.H., Lam, A.C.C. and Iu, V.P. (2004), "Experimental Investigation of Block Shear of Coped Beams with Welded Clip Angles Connection," *Proceedings, Fifth Structural Specialty Conference of the Canadian Society for Civil Engineering,* June 2–5.

APPENDIX A. TABLES

Table A1. Specimen Properties

Specimen	F_y (ksi)	E (ksi)	d (in.)	b_f (in.)	t_f (in.)	t_w (in.)	e (in.)	d_c (in.)	c (in.)
Cheng and Yura (1986)									
W1	39.4	29000[a]	17.9	6.00	0.439	0.304	4.00	1.25	3.50
W2	39.4	29000[a]	17.9	6.00	0.439	0.304	7.00	1.25	6.50
W3	39.4	29000[a]	17.9	6.00	0.439	0.304	10.5	1.25	10.0
RB18A	39.4	29000[a]	17.9	6.00	0.439	0.304	18.2	3.06	18.0
RB12A	57.3	29000[a]	11.9	3.97	0.239	0.212	9.09	1.25	8.90
RB12D	57.3	29000[a]	11.9	3.97	0.239	0.212	18.0	3.13	17.9
RB12B	55.3	29000[a]	12.0	4.00	0.239	0.217	12.2	1.13	12.0
RB12C	55.3	29000[a]	12.0	4.00	0.239	0.217	18.3	1.00	18.1
PB26A	59.4	29000[a]	26.5	6.00	0.181	0.132	13.1	1.13	13.0
PB26B	59.4	29000[a]	26.5	6.00	0.181	0.132	8.29	0.91	8.16
Ricles and Yura (Ref: Cheng and Yura, 1986)									
10–4	50.3	29000[a]	9.9	5.70	0.360	0.251	8.50	1.50	8.00
10–7	50.3	29000[a]	9.9	5.70	0.360	0.251	6.50	1.75	6.00
18–14	36.6	29000[a]	18.2	7.47	0.685	0.423	9.00	1.50	8.00
18–15	36.6	29000[a]	18.2	7.47	0.685	0.423	5.63	1.50	5.00
Yam et al. (2003)									
406d005	49.7	31400	15.7	5.50[a]	0.345[a]	0.250[a]	13.7	0.78	13.5
406d01	49.7	31400	15.7	5.50[a]	0.345[a]	0.250[a]	13.7	1.57	13.5
406d03	49.7	31400	15.7	5.50[a]	0.345[a]	0.250[a]	13.7	4.70	13.5
457d02	49.7	31400	17.7	6.00[a]	0.425[a]	0.300[a]	15.5	3.54	15.3
Birkemoe and Gilmor (1978)									
I-2	52.5	29000[a]	18.0[a]	7.50[a]	0.500[a]	0.305[a]	6.50	1.00	6.00
Zhong et al. (2004)									
A1	46.1	27700	15.9	5.55	0.437	0.268	5.12	1.29	3.94
A2	46.1	27700	15.9	5.55	0.437	0.268	5.91	1.22	4.73
B1	46.1	27700	15.9	5.55	0.437	0.268	5.12	1.18	3.94
B2	46.1	27700	15.9	5.55	0.437	0.268	6.30	1.18	5.12
D1	53.9	29500	18.0	7.45	0.559	0.362	7.09	1.18	5.91
E2	42.4	29500	14.3	6.75	0.598	0.358	5.12	1.18	3.94

[a] Nominal value

Table A2. Specimens Failing by Localized Buckling or Shear Yielding											
	Experiment		Cheng and Yura (1986)			Yam et al. (2003)			15th Ed. AISC Manual		
Specimen	R_e (kips)	EFM	R_c (kips)	$\frac{R_e}{R_c}$	PFM	R_c (kips)	$\frac{R_e}{R_c}$	PFM	R_c (kips)	$\frac{R_e}{R_c}$	PFM
Cheng and Yura (1986)											
W1	115	VY/IB	119	0.966	VY	119	0.966	VY	119	0.966	VY
W2	112	VY/IB	115	0.966	FY	119	0.935	VY	119	0.935	VY
W3[a]	99.0	IB	76.9	1.29	FY	109	0.905	LB	89.5	1.11	IB
RB18A[b]	46.5	IB	36.0	1.29	FY	43.2	1.08	LB	36.5	1.27	IB
RB12A	37.9	IB	28.8	1.32	LB	34.9	1.09	LB	28.8	1.32	EB
RB12D	12.9	EB	9.10	1.42	LB	13.4	0.959	LB	9.10	1.42	EB
RB12B	27.8	EB	20.6	1.35	LB	26.3	1.06	LB	20.6	1.35	EB
RB12C	16.8	EB	11.5	1.46	LB	15.7	1.07	LB	11.5	1.46	EB
PB26A	14.1	EB	6.88	2.05	LB	7.97	1.77	LB	6.88	2.05	EB
PB26B[c]	20.8	EB	14.9	1.39	LB	16.1	1.29	LB	14.9	1.39	EB
Ricles and Yura (Ref: Cheng and Yura, 1986)											
10–4	47.0	IB	27.9	1.68	FY	57.8	0.813	LB	38.9	1.21	IB
10–7	59.0	IB	34.5	1.71	FY	62.0	0.953	VY	51.7	1.14	IB
18–14	151	IB	122	1.24	FY	155	0.973	VY	155	0.973	VY
18–15	164	IB	155	1.06	VY	155	1.061	VY	155	1.06	VY
Yam et al. (2003)											
406d005	37.3	EB	35.3	1.06	LB	44.1	0.845	LB	35.3	1.06	EB
406d01	36.2	EB	32.6	1.11	LB	39.9	0.907	LB	32.6	1.11	EB
406d03	25.2	EB	25.5	0.988	LB	28.5	0.883	LB	25.5	0.988	EB
457d02	60.5	EB	43.5	1.39	LB	51.1	1.18	LB	43.5	1.39	EB
			Average	1.32			1.04			1.23	
			Standard deviation	0.288			0.218			0.267	

[a] For specimen W3, the inflection point was 3.9 in. from the beam end. Clip angles restrained buckling.
[b] For specimen RB18A, the inflection point was 8 in. from the beam end.
[c] Specimen PB26B failed by shear buckling with post-buckling capacity due to tension field action.

R_e = experimental beam end reaction

R_c = calculated beam end reaction

EFM: experimental failure mode
PFM: predicted failure mode

EB: elastic localized buckling
FY: flexural yielding
IB: inelastic localized buckling
LB: localized buckling
VY: shear yielding

Table A3. Specimens Failing by Block Shear Buckling							
Specimen	L/h_o	R_e (kips)	R_f (kips)	R_v (kips)	R_b (kips)	R_{min} (kips)	$\frac{R_e}{R_{min}}$
Birkemoe and Gilmor (1978)							
I-2[a]	0.353	112	220	163	122	122	0.918
Zhong et al. (2004)							
A1	0.431	88.8	177	108	86.3	86.3	1.03
A2	0.375	98.3	146	109	94.0	94.0	1.05
B1	0.321	88.6	179	109	74.6	74.6	1.19
B2	0.294	87.7	134	109	98.8	98.8	0.888
D1	0.282	140	279	196	155	155	0.903
E2	0.360	131	239	119	107	107	1.22
						Average	1.03
						Standard deviation	0.126

[a] The bolt bearing strength for specimen I-2, according to AISC Specification Equation J3-6b, is 163 kips.

R_e = experimental beam end reaction
R_f = calculated beam end reaction for the limit state of flexure, based on the revised AISC *Manual* design procedure
R_v = calculated beam end reaction for the limit state of shear yielding
R_b = calculated beam end reaction for the limit state of block shear
R_{min} = minimum of R_f, R_v and R_b